Creep-Fatigue Interaction on Thermina Samples Experimental and Numerical Results

M. T. Cabrillat, Ph. Martin
CEA-CEN Cadarache, St. Paul-lez-Durance, France

1. INTRODUCTION

The Thermina tests are part of an experimental program which CEA has undertaken during the last few years in order to study the problems of creep/fatigue interaction on structures operating at high temperature in reactors.
An other paper (ref. 1) presents more precisely the objectives of this global experimental program including several tests, together with the lessons drawn from a design point of view.
The present article presents the Thermina experimental program, describing the test carried out and the calculations performed to interpret them.

2. DESCRIPTION OF THE TEST

The Thermina test was specially designed to study the problems of creep-fatigue interaction in presence of primary constant loading and secondary cyclic loading.
The principle of the tests was presented in a previous SMIRT (ref. 2). Figure 1 shows the testing configuration used and figure 2 is a diagram of the samples tested.
The samples were subjected to a primary axial force which was kept constant for a given test as well as to sodium thermal shocks. The samples were filled with sodium and were maintained at 600°C by means of an electrical heater. The thermal shock was realized by sending cold sodium (θ cold) on the outer surface of the sample for 20 seconds by means of an immerged electromagnetic pump. The temperature of the sample then returned to 600°C and remained at this value for a hold period, T_M, before being subjected to the next shock.
Two different sample geometries were defined so that only membrane stresses appear in type 1 samples in presence of an axial force while significant bending stresses occur in type 2 samples.
Because the samples are comparatively small, it is possible to use four devices at the same time and thus to test four samples in each test series.

3. TESTS PERFORMED

At the present time, 5 series of tests have been carried out. Each series comprises 4 samples of which 2 are symmetrical (type 1) and 2 asymmetrical (type 2). The primary loads applied to the 4 samples were assumed to be identical.
For the first two series of samples, the primary loading was evaluated relatively to elastic calculations. The following standard relations were adopted ; P being a stress value :
σVM membrane (at plate to shell junction) = P for the symmetrical samples.
σVM membrane + bending (at lower plate to shell junction) = 1.5 P for the asymmetrical samples of the same series.
But when the interpretation calculations were carried out (see ref. 1), we observed that the bending stresses caused by the axial force were not of a primary nature. Therefore in the remainder of the tests, the samples were subjected to an axial force such that :
σVM membrane = imposed P at the plate to shell junction (lower junction for asymmetrical samples).
A summary of the test conditions in the 5 series is given in the following table.

SAMPLES	SERIES A	SERIES B	SERIES C	SERIES D	SERIES E
Test conditions					
Θ hot	600°C	600°C	600°C	600°C	600°C
Θ cold	400°C	400°C	400°C	300°C	300°C
Imposed P	140 MPa	100 MPa	50 MPa	100 MPa	100 MPa
T_H	6 h	6 h	6 h	2 h	2 h

On and after series D, the amplitude of the thermal shocks was increased and the period of hold time at 600°C was changed from 6 hours to 2 hours in order to increase fatigue damage relatively to creep damage.

4. EXPERIMENTAL RESULTS

The following table shows the number of cycles undergone by each sample during the tests.

	Sample 1 Symmetrical	Sample 2 Asymmetrical	Sample 3 Symmetrical	Sample 4 Asymmetrical
Series A	340	110	107	265
Series B	358	300	343	315
Series C	650	596	526	644
Series D	589	573	645*	645
Series E	302	302	452	431*

* indicates samples broken during the tests.

It thus appears that increasing the thermal loading causes significant damage in a relatively short time. It will be then possible to cause an extensive range of damage by varying the loading parameters or the number of cycles imposed. This will be of interest when testing different types of damage modeling.
Metallurgical analyses were performed on these samples in order to characterize the nature of the damage experienced. These tests have not yet been completed. Fractographic examination was carried out on series A, B and C together with micrographic examination using an electron scan microscope. Partial observations using the electron scan microscope were also carried out on test piece D3 which broke during testing.
The results of all these tests are purely qualitative. The internal skin of all the samples showed incipient intergranular cracks in the area of the plate to shell groove ring. These cracks developed more or less for the different samples. Smallest cracks of about 150 μm were observed in sample A3 for instance which sustained few cycles while through wall cracks were obtained on series D.
Between these two extreme values, cracks of intermediate length were observed on other samples.
Fig. 5 shows results obtained on B3 sample after 343 cycles : one main crack is observed all together with crack initiations at grain boundaries.
The fractographs revealed an internal area with numerous integranular decohesions and creep cavities. A more ductile area including dimples was observed on the exterior. The extent of the intergranular area varied from sample to sample. In sample D3, the intergranular area constituted 4/5 of the thickness, the remaining ligament broke suddenly due to the effect of the primary stress and was thus proved to be ductile in character (fig. 4). The intergranular area was smaller in the other samples.
For purposes of comparison, a fractograph was taken of a test piece that had not been subjected to any stress. In this case, breaking was entirely ductile with dimples and the test piece underwent significant cross-sectional contraction when tensile force was applied, leading to breaking. In contrast, the test pieces tested in sodium underwent practically no deformation when the same tensile force was applied. They appeared to have lost a considerable amount of ductility.
Similar observations were made during creep tests carried out on samples taken on the one hand from a new test piece and on the other, from sample A1 after testing in sodium. Creep ductility in test piece A1 was twice lower than that of a new test piece (fig. 3).

These creep tests also revealed the effect of multiaxial stress on creep life. Creep life is twice longer in samples which include the core of the test piece than in smooth uniaxial samples (without geometric discontinuities).

5. CALCULATIONS

A large number of calculations were performed to interpret the test and to evaluate the conservatism of the different methods of analysis. The calculations concerned the loading in series A, B and C (θ Na = 600°-400°C, T_H [Hold Time] = 6 hours).
In order to obtain the thermal fields throughout the structure during the various transients, thermal calculations in conduction were performed. It was necessary to take the conduction of sodium contained in the samples into account in order to obtain good agreement between the calculations and the measurements made during the tests. In fact, sodium has a higher thermal conductivity than steel. It therefore cools faster during thermal shock, thereby contributing to the cooling of the sample.

5.1 Elastic calculations

a) RCCMR analysis

The elastic calculations showed that stresses were maximum in the internal skin of the samples and at the junction between the plate and the shell. it was indeed in these areas that all the cracks started.
The first analyses were carried out according to the rules of the RCCMR, 1985 edition. This method gave us the following N_R initiation cycle numbers :

Imposed P MPa	0	50	100	140
Design curves N_R	3	1	< 1	< 1
Best fit curves N_R	75	14	2	1

But since the purpose of the experimental program was to improve design rules, the tests contributed to propose new rules which were included in the RCCMR addition in 1987 (ref. 1).
Application of these new rules to Thermina tests give the following predictions :

Imposed P MPa	0	50	100	140
Design curves N_R	16			2
Best fit curves N_R	310	212	115	62

These results seem to present good agreement with the experimental results.

b) Test of other damage law

We used the results of the elastic calculations to test other types of damage laws. In particular, we used the model developped by J. Lemaître and J.L. Chaboche (ref. 3).
In this model, fatigue and creep damage are coupled on the assumption of additivity of damages. this assumption allows the following physical effects to be taken into account :
- the presence of creep damage accelerates the progress of fatigue microcracks,
- the presence of fatigue cracks increases the growth rate of creep cavities due to the concentration of stress effect.

Application of this damage model to the Thermina test gave us the following initiation cycle numbers :

Imposed P MPa	0	50	100	140
N_R	96	75	57	44

This model yielded predictions which were slightly more severe than those of the RCCMR and which were in particular less sensitive to variations in primary stress. This is probably due to problems in fitting the parameters of the damage law. Optimization of these parameters should enable the predictions given by this model to be improved.

5.2 Inelastic calculations

Inelastic calculations were performed for the different primary loads using the following constitutive models :

- elastoplastic calculation with a linear kinematic model identified on the reduced cyclic curves,
- elastoplactic calculations using a non-linear kinematic model (Chaboche model with 3 parameters : 1 kinematic variable, no isotropic hardening) (ref. 3),
- viscoplastic calculation with plasticity and creep combined. The plastic model used in this calculation was the linear kinematic model. The creep law used was the primary creep law with time hardening assumption identified by EDF using cyclic relaxation tests on material cycled at $\Delta\varepsilon_T$ = 0.7 % and at 600°C.

The two plastic models used gave somewhat different results. In the Thermina samples, the hold time does not occur at the moment of maximum stresses (approximately 1 second after the start of the thermal shock) but in a state of residual stress on returning to the isothermic state.
Figure 6 summarizes the differences in behavior of the two models for the two extreme load cases for which calculations were performed. The results are given at the junction between the plate and the shell, on the inner face.
The Chaboche model tends to make the cycles symmetrical. It therefore gives stresses at the residual state which :

- are higher than those obtained with the linear kinematic model,
- are less sensitive to the primary stress value.

In the linear kinematic model, the cycles obtained for the different primary loads are similar, the primary stress only causing a shift in the cycles towards traction. However, in the cases where imposed P = 140 MPa, the two plastic models gave virtually the same values for residual stress at start of hold time.
The consequences for estimated creep and fatigue life are important. The linear kinematic model for low levels of primary stress give low levels of stress during hold time and thus low creep damage. Fatigue damage becomes more important.
Numbers of initiation cycles were estimated following the 1985 RCCMR rules, i.e. using the linear cumulative damage model without taking relaxation of stress during hold time into account.
The following results were obtained using these hypotheses :

Imposed P MPa	Linear Kinematic Model		Chaboche Model	
	Design curves	Best fit curves	Design curves	Best fit curves
140	$N_R = 3$ Df = 0 Dc = 1	$N_R = 65$ Df = 0.01 Dc = 0.98	$N_R = 2$ Df = 0 Dc = 1	$N_R = 40$ Df = 0 Dc = 1
100	$N_R = 12$ Df = 0.03 Dc = 0.9	$N_R = 230$ Df = 0.03 Dc = 0.92	$N_R = 3$ Df = 0 Dc = 1	$N_R = 58$ Df = 0 Dc = 1
50	$N_R = 80$ Df = 0.22 Dc = 0.48	$N_R = 1080$ Df = 0.15 Dc = 0.65	$N_R = 4$ Df = 0.01 Dc = 1	$N_R = 100$ Df = 0.01 Dc = 1
0	$N_R = 240$ Df = 0.67 Dc = 0.14	$N_R = 3100$ Df = 0.43 Dc = 0.23	$N_R = 10$ Df = 0.02 Dc = 1	$N_R = 160$ Df = 0.02 Dc = 0.96

with Df = fatigue damage
and Dc = creep damage

Calculations using the viscoplastic model (linear kinematic and creep combined) enable the evolution of stress during hold time to be included. They give the following results :

Imposed P MPa	Viscoplastic calculations			
	Design curves		Best fit curves	
140	$N_R = 6$	Df = 0.02 Dc = 1	$N_R = 130$	Df = 0.04 Dc = 0.98
100	$N_R = 15$	Df = 0.04 Dc = 0.93	$N_R = 310$	Df = 0.04 Dc = 0.90

It will be seen that the linear kinematic model tends to become non-conservative for low primary stresses. Without taking relaxation of stress during hold time into account, 1080 initiation cycles are planned when primary stress equals 50 MPa, whereas the corresponding samples (series C) already have incipient cracks 200 µm deep after 500 cycles. This is due to the fact that the linear kinematic model under estimates the stresses in the residual state for off-center deformation cycles. Conversely, if hold time were at the peak of the cycle, there would be a tendency to overestimate the stresses by preventing for relaxation of the mean stress and would thus also overestimate the damage.

CONCLUSIONS

The Thermina experimental program was undertaken to study the problems of creep fatigue interaction in structures. It has already contributed to the improvement of elastic analysis methods used by RCCMR (ref. 1). The new analysis routines enable to predict initiation cycle numbers which appear to be in good agreement with experimental results.
From an experimental point of view, through wall cracks occurred during testing. It is therefore now possible to produce an entire range of damage, for example by carrying out interrupted tests or by modifying loading parameters.
The first metallurgical analyses have enabled damage to be characterized. The next step will consist of attempting to quantify this damage in order to establish correlations with loading and to test various damage models.
As far as the constitutive equations models are concerned, the linear kinematic model appears to underestimate the stresses (and hence the damage) in low primary stresses. More sophisticated models are required to give correct predictions in all loading situations.

REFERENCES

/1/ M.T. CABRILLAT - Ph. MARTIN
Assessment of the creep fatigue damage by the elastic route of the RCCMR.
Some lessons drawn from in sodium tests.
SMIRT 10. Division E. California U.S.A., August 1989.

/2/ M.T. CABRILLAT - J.L. CARBONNIER - G. CORDIER
Creep-fatigue interaction in small mock-ups submitted to thermal shocks and primary stresses.
SMIRT 8. Paper L7/2, Brussels, August 1985.

/3/ J. LEMAITRE - J.L. CHABOCHE
Mécanique des matériaux solides, Dunod 1985.

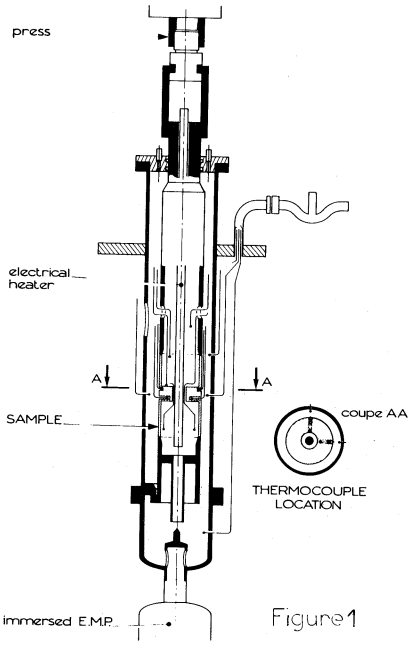

Figure1

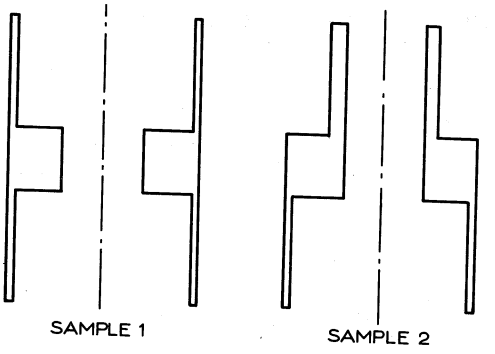

figure 2

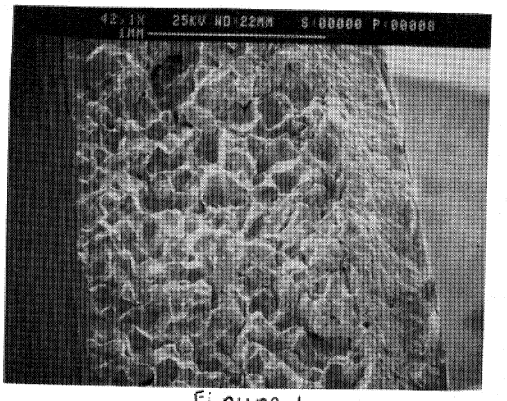

Figure 4

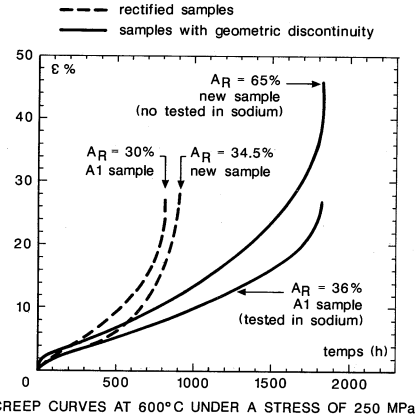

CREEP CURVES AT 600°C UNDER A STRESS OF 250 MPa

Figure 3

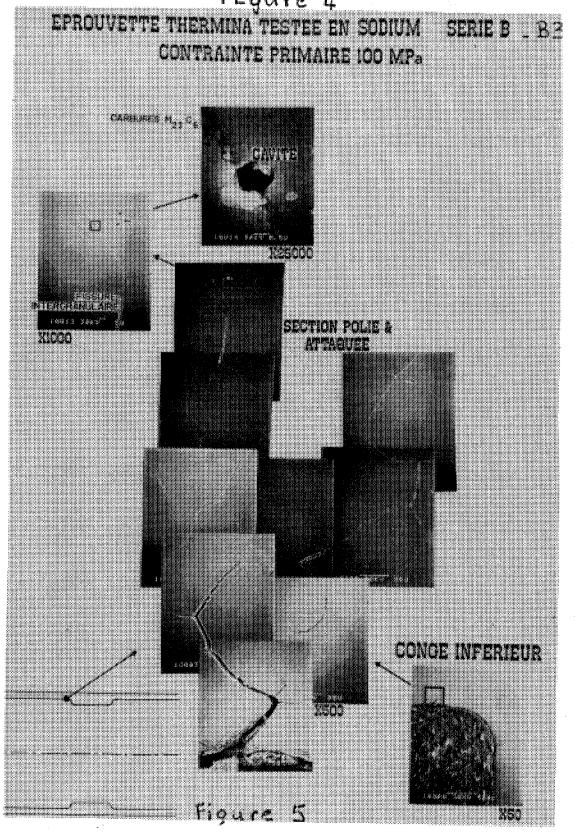

Figure 5

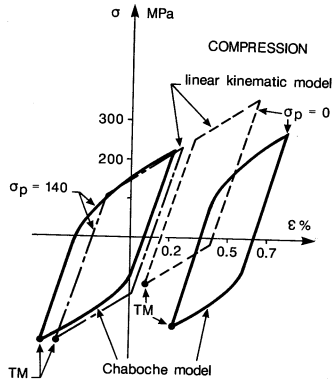

TM : hold time position

Figure 6